SUPPLEMENTAL MATERIAL

Nexilin is a New Component of Junctional Membrane Complexes Required for Cardiac T-tubule Formation

Canzhao Liu, MD, PhD[1*]; Simone Spinozzi, PhD[1*]; Jia-Yu Chen, PhD[2]; Xi Fang, PhD[1]; Wei Feng, MD, PhD[1]; Guy Perkins, PhD[3]; Paola Cattaneo, PhD[4,5]; Nuno Guimarães-Camboa, PhD[6,7]; Nancy D. Dalton, RDCS[1]; Kirk L. Peterson, MD[1]; Tongbin Wu, PhD[1]; Kunfu Ouyang, PhD[8]; Xiang-Dong Fu, PhD[2,9]; Sylvia M. Evans, PhD[1,10]; Ju Chen PhD[1]

[1]Department of Medicine, University of California San Diego, La Jolla, CA 92093, USA.
[2]Department of Cellular and Molecular Medicine, University of California San Diego, La Jolla, CA 92093, USA.
[3]National Center for Microscopy and Imaging Research, University of California San Diego, La Jolla, CA 92093, USA.
[4]National Research Council, Institute of Genetics and Biomedical Research, Milan 20138, Italy.
[5]Humanitas Clinical and Research Center, Rozzano 20089, Italy.
[6]Institute for Cardiovascular Regeneration, Centre of Molecular Medicine, Goethe University Frankfurt, 60590 Frankfurt, Germany.
[7]German Center for Cardiovascular Research DZHK, Berlin 13347, Germany.
[8]Drug Discovery Center, State Key Laboratory of Chemical Oncogenomics, School of Chemical Biology and Biotechnology, Peking University Shenzhen Graduate School, Shenzhen 518055, China.
[9]Institute of Genomic Medicine, University of California San Diego, La Jolla, CA 92093, USA.
[10]Department of Pharmacology, Skaggs School of Pharmacy and Pharmaceutical Sciences, University of California San Diego, La Jolla, CA 92093, USA.
[*]These authors contributed equally to this work and are listed in alphabetical order.

Supplemental Methods

Supplemental Table 1: List of primers used.

Supplemental Table 2: List of antibodies used.

Supplemental Table 3: Transthoracic echocardiography values related to Fig.2.

Supplemental Figure 1: Global loss of NEXN leads to progressive and severe dilated cardiomyopathy.

Supplemental Figure 2: Intracardiac thrombus in dilated NEXN gKO hearts.

Supplemental Figure 3: The cardiac specific Cre recombinase activity of Xenopus laevis myosin light-chain 2-Cre mice.

Supplemental Figure 4: Echocardiographic analysis of Xenopus laevis myosin light-chain 2-Cre mice.

Supplemental Figure 5: Phenotype evaluation of troponin T2-cre $NEXN^{f/f}$ mice.

Supplemental Figure 6: Quality control of RNA-seq data.

Supplemental Figure 7: Expression of Calsequestrin 2 in Nexn cKO heart.

Supplemental Figure 8: NEXN does not localize in the Z-disc of P5 cardiomyocytes and sarcomere structure is not altered by loss of NEXN.

Supplemental Figure 9: NEXN protein level in induced heart disease mouse model.

Supplemental Movie: Tridimensional reconstruction from representative Micro-CT images of a P10 *Nexn* KO showing 4 and 2 chamber section views revealing a complex structure attached at the anterior wall of the left ventricle.

Supplemental Materials & Methods

Generation of Nexilin mice

The construct of Nexilin (*Nexn*) was generated in the pDLNL vector in three sections as previously described[1] (Fig. S1). The 5′ arm of homology consisted of a 7-kb ApaI fragment that was generated using the primers forward, 5′- CACTGCTCGAGGGGGGTGACTCTAGAGCTTGCCCATT-3′; and reverse, 5′- TTGATATCATGCATGCAGCCAGGGATACACAGAGAAA-3′. The middle fragment containing the first LoxP site, neomycin, flanked by the flippase recombination target sites exon 1 to exon 4 and the second LoxP site was generated using the primers forward, 5′- CAAGCTCCGGGGATCGCCTGCCCGGCTCCTGGAACTCACTTTGTAGAC-3′; and reverse, 5′- TAGGAACTTCGGATCCTACTGGGCAACGGACGTGAA -3′. The 3′ arm consisted of a 5.3-kb SalI fragment that was generated using the primers forward, 5′- ATCCTCTAGAGTCGATATGGGCAGAATGGGCCTAT-3′; and reverse, 5′- CCCCCTCGAGGTCGACTTGGGCACAGGAATGGATTAC-3′. Both targeting constructs were verified by sequencing and linearized with NotI before electroporation into ES cells at the Transgenic Core Facility at the University of California San Diego. G418-resistant ES clones for *Nexn* were screened for homologous recombination by Southern blotting as described. Global loss of *Nexn* in mice were generated by crossing floxed *Nexn* mice (with *Sox2*-cre deleter mice, and cardiomyocyte-specific knockout (cKO) mice by crossing floxed *Nexn* (*Nexn*$^{f/f}$) mice with Xenopus laevis myosin light-chain 2 cre mice (XMLC2-cre) and troponin T2 cre mice (cTNT-Cre). The corresponding littermate controls were *Nexn*$^{f/f}$; XMLC2-Cre-negative mice or *Nexn*$^{f/f}$; cTNT-Cre-negative mice. XMLC2-Cre-positive mice were analyzed by transthoracic echocardiography to evaluate the Cre toxicity (Fig. S4).

Animal procedures and echocardiography

The UCSD Animal Care Program maintained all animals and the UCSD Institutional Animal Care and Use Committee approved all experimental procedures. Genotyping was performed using primer reported in Table S3. For echocardiography, adult mice were anesthetized with 5% isoflurane for 15 seconds and maintained at 0.5% isoflurane during the procedure. Echocardiography was performed by using a VisualSonics, SonoSite FUJIFILM, Vevo 2100 ultrasound system with a linear transducer 32-55MHz. Percentage fractional shortening (%FS) was used as an indicator of systolic cardiac function. Measurements of left ventricular (LV) internal diameter at end-diastole (LVIDd) and LV internal diameter at end-systole (LVIDs) were determined from the M-mode tracing. For embryonic and neonatal mice no anesthesia was used, animals were gently held in place on a heated platform. Embryos (E18.5) were resuscitated after a caesarian-cut and maintained at 37°C. Echocardiography at E18.5 was performed after the mice started to properly breath and move.

Neonatal/embryonic cardiomyocytes, plasmids and adenoviral vectors

Neonatal mouse cardiomyocytes were prepared as previously described[2] and maintained in Dulbecco's modified Eagle's medium (DMEM) supplemented with 10% horse serum, 5% fetal bovine serum (FBS), 100 U/mL penicillin and 100 µg/mL streptomycin for 24 hours before adenovirus infection. Mouse *Nexn* and *Jph2* cDNA were amplified by PCRs using KOD polymerase (Emd Millipore) and subcloned into p-EGFP-C1 or 3xFlag-pcDNA3 vectors with Bgl II and Hind III or Hind III and XbaI sites using an In-Fusion® HD Cloning Plus kit (takara). Adenoviruses expressing cre and lacZ were obtained from the UCSD Viral Vector Core.

Adult cardiomyocyte isolation

The heart was removed following isoflurane anesthesia and rinsed in Krebs-Henseleit buffer B (KHB-B) (118 mM NaCl, 4.8 mM KCl, 25 mM HEPES, 1.25 mM K2HPO4, 1.25 mM MgSO4, 11 mM glucose, pH 7.4). The heart was cannulated through the aorta and perfused on a Langendorff apparatus with KHB solution (3 ~ 5 minutes, 37 °C), then incubated with KHB enzyme solution (1.5 mg/ml

Collagenase Type 2, 25 µM Blebbistatin) for 12 minutes at 37 °C. After digestion, the heart was perfused with 5 ml KHB solution to wash out the collagenase. Then the hearts were minced in KHB solution with 2% BSA, gently agitated, then filtered through a 100µm polyethylene mesh. After settling, cells were re-introduced to calcium against a concentration gradient (100 uM/200 uM/500 uM/1 mM) and stored in KB solution at room temperature before use.

NEXN polyclonal antibody production and purification

The epitopes against NEXN N-terminus (15~30: CKPVPKSYVPKLGKGD), the central part (177~190: CKSYKTPGKTKDPED) and C-terminus (567~579: CEDEEQTRSGAPWF) were designed and synthesized. The customized antibodies were generated by YenZym Antibodies using the epitopes described above. The serum resulting from the NEXN N-terminus immunization was then purified with the Antibody Serum Protein A-Purification Kit (Abcam, ab109209) following the manufacturer's instructions.

Whole heart imaging and butterfly cut

Hearts were fixed in 4%PFA and embedded in an agarose 10% matrix. Afterwards, a butterfly cut was performed on a subset of samples for a gross intra-anatomical evaluation. Heart images were acquired in a stereomicroscope (Olympus, SZX12). The resulting pictures were cleared and processed with Photoshop CC (Adobe) in order to remove the uninformative feature of the surrounding agarose matrix without altering the features of the heart shape and structure.

Histology and immunofluorescence

Hearts were perfused with PBS and fixed overnight in PFA4%/PBS. Afterwards, the fixed samples were embedded in OCT tissue tek (Sakura) or dehydrated and embedded in paraffin. Sections were cut between 5 and 10 µm thickness. Sections for histology were stained with kits for Masson trichrome (Sigma-Aldrich HT15), Vernhoff Van Gieson (Sigma-Aldrich HT25A), or Carstairs (EMS, 26381) staining following the manufacturer's instructions, and then images were acquired with a Hamamatsu Nanozoomer 2.0HT Slide Scanner. For Immunofluorescence, sections or isolated cardiomyocytes were blocked in 10% Goat serum/PBS before incubation with antibodies. The antibodies were diluted in a 2% bovine serum albumin solution in PBS. Primary and secondary antibodies are listed in Table S4.

Immunofluorescence images were acquired using a Zeiss LSM 880 airy scan confocal microscope. Image processing were performed with Fiji software and Photoshop CC (Adobe).

T-tubule imaging

Isolated cardiomyocytes were incubated with 50µM Di-8 Anepps (Thermo Fisher Scientific, D3167) for 20 minutes on matrigel (Millipore Sigma, E6909) coated chamber imaging slides (Ibidi). After 2 quick washes, the cells were analyzed using a Zeiss LSM 880 airy scan confocal microscope with an excitation at 458nm and a detection spectrum between 550nm and 740nm as previously described[3].

Micro-CT scan

Hearts from *Nexn* gKO mice and WT littermates were perfused in PBS and fixed overnight in 4%PFA in PBS. The samples were analyzed with the nanoCT system GE Phoenix Nanotom M by the Molecular Imaging Center at the University of Southern California. The resulting images were processed with VG studio Max (Volume Graphics) and Fiji software[4] for section pictures and with Arivis Vision4D software (Arivis AG) for the creation of the tridimensional movie. QuickTime Player (Apple Inc.) was used for video trimming and format change.

RNA-seq data analysis

RNA-seq reads were mapped against the Ensembl v91 mouse gene model (GRCm38) for counting reads and estimating gene expression as described by Salmon[5]. The DEseq2 package[6] was used to

evaluate the reproducibility and perform differential gene expression analysis. Reads counts were normalized and rlog transformed for distance clustering (Fig. S6A and B) and principle component analysis (Fig. S6C). Differentially-expressed genes were detected by default setting of DESeq2. We specified the apeglm method to shrink the log2 fold change[7], and Benjamin-Hochberg algorithm to adjust p-value (www.jstor.org/stable/2346101). Fold changes > 1.5 or < 2/3 and adjusted p-value < 0.05 were then used to select differentially-expressed genes.

GO enrichment analysis

Gene list enrichment analyses were done using DAVID (https://david.ncifcrf.gov/). If present, only the top 5 significant entries in GOTERM_BP_3 and GOTERM_MF_5 (adjusted p-value cutoff: 0.05) were shown. The number of genes in each entry was also indicated (Fig. 3B, E).

Quantitative real-time PCR

Total RNA was prepared from heart tissue of *Nexn* cKO and control littermates using the TRI Reagent (Sigma-Aldrich). RNA molecules were reverse transcribed using Superscript III Reverse Transcriptase kits (Invitrogen) according to the manufacturer's instructions. The PCR mixture contained 1 µl diluted cDNA, 5 µl 2× iTaq Universal SYBR Green Supermix (BIO-RAD), and 200 nM of each gene-specific primer in a final volume of 10 µl. The real-time PCRs were performed using a Fast 96-Well System (Applied Biosystems). The primer sequences are reported in Table S3.

Protein isolation and Western Blot analysis

Total protein extracts were prepared by suspending ground heart tissue in Urea lysis buffer (8M Urea, 2M Thiourea, 3% SDS, 75 mM DTT, 0.03% Bromophenol Blue, 0.05 M Tris-HCl, pH 6.8). Isolated cardiomyocytes were lysed in RIPA solution (50 mM Tris, 10 mM EDTA, 150 mM NaCl, 0.25% Deoxycholic acid, 0.1% SDS, 2% NP-40 substitute, 0.01% Sodium azide). Protein lysates were separated on 4-12% SDS-PAGE gels (Life Technologies) and transferred for 2 hours at 4°C on to a PVDF membrane (BioRad). After blocking for an hour in 5% dry milk, membranes were incubated overnight at 4°C with the primary antibody (listed in Supplementary Table 4) in blocking buffer. Blots were washed and incubated with horseradish peroxidase (HRP)-conjugated secondary antibody generated in Rabbit (1:5000) or Mouse (1:5000) (Dako) for 1.5 hours at room temperature. Immunoreactive protein bands were visualized using an enhanced chemiluminescence reagent (Thermo Fisher Scientific).

Mass spectrometry

Dried samples were reconstituted with 2% acetonitrile, 0.1% formic acid and analyzed by LC-MS/MS using a Proxeon EASY nanoLC system (Thermo Fisher Scientific) coupled to a Q-Exactive Plus mass spectrometer (Thermo Fisher Scientific). Peptides were separated using an analytical C_{18} Acclaim PepMap column 0.075 x 250 mm, 2µm particles (Thermo Fisher Scientific) in a 93-min linear gradient of 2-28% solvent B at a flow rate of 300nL/min. The mass spectrometer was operated in positive data-dependent acquisition mode. MS1 spectra were measured with a resolution of 70,000, an AGC target of 1e6 and a mass range from 350 to 1700 m/z. Up to 12 MS2 spectra per duty cycle were triggered, fragmented by HCD, and acquired with a resolution of 17,500 and an AGC target of 5e4, an isolation window of 2.0 m/z and a normalized collision energy of 25. Dynamic exclusion was enabled with duration of 20 sec.

All mass spectra were analyzed with MaxQuant software version 1.5.5.1. MS/MS spectra were searched against the *Mus musculus* Uniprot protein sequence database (version July 2016) and GPM cRAP sequences (commonly known protein contaminants). Precursor mass tolerance was set to 20ppm and 4.5ppm for the first search where initial mass recalibration was completed and for the main search, respectively. Product ions were searched with a mass tolerance 0.5 Da. The maximum precursor ion charge state used for searching was 7. Carbamidomethylation of cysteines was searched as a fixed modification, while oxidation of methionines and acetylation of protein N-terminal were

searched as variable modifications. Enzyme was set to trypsin in a specific mode and a maximum of two missed cleavages was allowed for searching. The target-decoy-based false discovery rate (FDR) filter for spectrum and protein identification was set to 1%. Fold change of MS/MS spectral counts was used for identification of differential protein between wild type and *Nexn* cKO. Considering that lower number of MS/MS spectral counts provides a highly-variable estimation of fold change, while higher count number provides a more robust estimation, we applied a count-dependent rather than a static cutoff. Briefly, MS/MS spectral counts were first normalized by library size using DESeq2 for fold change estimation. These data were then grouped into 40 equally-spaced bins based on the range of $\log_2$-transformed average counts across all 8 samples. For each bin, we estimated the mean and variance of fold change for pinpointing the Z-score = ±1.5. LOESS local regression was applied to z-score = -1.5 or z-score = 1.5 data points, separately. Any protein with its fold change of MS/MS spectral counts out of range of z-score = (-1.5,1.5) will be considered as being differentially regulated between wild type and *Nexn* cKO.

Calcium imaging

Cardiomyocytes isolated from hearts were incubated with 2 μM Fluo-4 AM (Thermo Fisher Scientific) in Tyrode calcium-free solution for 30 minutes at room temperature. The cells were washed with normal Tyrode solution (1.8 mmol/L Ca^{2+}) for 20 minutes for de-esterification and subsequently imaged by confocal microscopy[8]. Line scans were used to obtain calcium transient amplitudes. Data were analyzed using ImageJ and the SparkMaster plug-in. The amplitude of intracellular Ca2+ transients was determined by the change between the basal and peak ratio (ΔF/F0). The decay portion of the calcium transient (time to 63% decline) was used to measure the calcium decay (Tau).

Immunoprecipitation

NEXN was immunoprecipitated from WT mouse heart (3 weeks) tissue lysates using a customized NEXN antibody (epitope against middle region of NEXN). Rabbit non-specific IgG (Santa Cruz) and beads (Thermo Scientific) were used as negative controls. After washing 3 times with IP lysis buffer, beads were incubated with 2× Lamelli buffer at 70 ℃ for 10 minutes then gel electrophoresed and immunoblotted.

For co-IP from HEK cells, cell lysates were rotated overnight at 4°C in 500 μL of IP lysis buffer with 20 μL of monoclonal anti-GFP antibody (Santa Cruz). Murine IgG nonspecific antibody was used as a negative control. Next, 30 μL of PBS-washed protein G beads (Thermo Scientific) Beads were resuspended and incubated in lysate–antibody complexes for 1 hour at 4°C. After washing 3 times with IP lysis buffer, beads were incubated in 2× Lamelli buffer for 10 minutes at 70°C. The immunoprecipitates and input lysate were gel electrophoresed and immunoblotted with the antibodies indicated in the paper.

Electron microscopy

Left ventricular tissue was extracted from hearts of E18.5 *Nexn* cKO mice and littermate CTRLs and washed in PBS. After a 1-hour pre-fixation in 2% paraformaldehyde + 2.5% glutaraldehyde in 0.1 M sodium cacodylate buffer pH 7.4, the samples were post-fixed in 1% osmium tetroxide. The samples were than stained overnight in 2% uranyl acetate and dehydrated in graded ethanol solutions and embedded in Durcupan ACM (Sigma). Sections were cut between 50 and 70 nm thick and images were recorded on a FEI Technai 12 Spirit electron microscope operated at voltages ranging from 80 to 120 kV. Images were randomly acquired in the cardiomyocyte's peripheral areas containing sarcolemma and sarcoplasmic reticulum in order to evaluate JMCs. Distances in MCSs between PM and SR were measured using Fiji software. For quantification purposes 2 different groups were created: i. gap size of ~12nm (all contact sites with a membrane distance between 10nm and 15nm) and ii. gap size of ~30nm (all contact sites with a membrane distance between 26nm and 32nm).

Supplemental Table 1. List of primers used.

Primers	5’-3’	Application
NX-F	5’-TCAAAGGGAAGGTCATTAAAATTC-3’	Mice genotyping
NX-R	5’-TGATGATGATGATGTTGCTAAGTG-3’	Mice genotyping
Cre-F	5’-GTTCGCAAGAACCTGATGGACA-3’	Mice genotyping
Cre-R	5’-CTAGAGCCTGTTTTGCACGTTC-3’	Mice genotyping
Rrad-F	5’-CAGAGGAGGGCGTTTACAAG-3’	qRT-PCR
Rrad-R	5’-TTCTGCTTCAGGTCCGTCTT-3’	qRT-PCR
Casq1-F	5’-GAATCCACATTGTCGCCTTT-3’	qRT-PCR
Casq1-R	5’-GTCGGGGTTCTCAGTGTTGT-3’	qRT-PCR
Atp2a2-F	5’-TACTGACCCTGTCCCTGACC-3’	qRT-PCR
Atp2a2-R	5’-CACCACCACTCCCATAGCTT-3’	qRT-PCR
Jph2-F	5’-ATCAAGGCCAATTCACCAAC-3’	qRT-PCR
Jph2-R	5’-GCAGCGAGGACAGAGAAGTG-3’	qRT-PCR
Cacna2d1 -F	5’-CAGCAACGCTCAGGATGTAA-3’	qRT-PCR
Cacna2d1 -R	5’-ATCTGTGATCCCCTTTGCTG-3’	qRT-PCR
Bin1-F	5’-ATGAAGCCAAAATTGCCAAG-3’	qRT-PCR
Bin1-R	5’-CGGAGCAGGTTAGTTTGAGC-3’	qRT-PCR
Ryr2-F	5’-ATTGACTTGCCCATCGAGTC-3’	qRT-PCR
Ryr2-R	5’-TGTTCTGCTTGTCCTCATGC-3’	qRT-PCR
Cacna1c-F	5’-AGAGGGAGAAAGCCAAAGCC-3’	qRT-PCR
Cacna1c-R	5’-TCGGGGTCAATGTCTTCTGC-3’	qRT-PCR

Supplemental Table 2. List of antibodies used.

Antibody	Source, Cat. No	Antibody	Source, Cat. No
RyR2	ENZO, ALX-804-016-R100	Cacna2d1	abcam, ab2864
JPH2	Santa Cruz, sc-51313	Casq1	Santa Cruz, sc-28274
Flag	Sigma-Aldrich, F1804	SERCA2	Santa Cruz, sc-73022
Bin1	abcam, ab185950	PLN	Thermo Scientific, MA3-922
GAPDH	Santa Cruz, sc-32233	α-actinin	Sigma-Aldrich, A7811
Myomesin	DSHB, B4	GFP	Santa Cruz, sc-9996
mouse-A647	Thermo Scientific, A31571	mouse-HRP	Dako, P0161
rabbit-A488	Thermo Scientific, A21206	rabbit-HRP	Dako, P0448
goat-A546	Thermo Scientific, A11056	goat-HRP	Dako, P0449
Cacna1c	alomone labs, ACC-003		

Supplemental Table 3. Transthoracic echocardiography values related to Fig.2.

Age	Genotype	HR (bpm)	LVIDd (mm)	LVIDs (mm)	%FS	LVPWd (mm)
P1	CTRL	255	1,05	0,66	37,1	0,37
P1	CTRL	314	1,00	0,54	46,4	0,35
P1	CTRL	323	0,85	0,48	43,6	0,30
P1	CTRL	297	0,84	0,50	40,2	0,33
P1	CTRL	270	1,02	0,60	41,1	0,33
P1	CTRL	299	0,91	0,65	28,0	0,39
P1	cKO	337	1,15	0,85	25,4	0,34
P1	cKO	410	0,81	0,54	33,7	0,35
P1	cKO	364	0,76	0,56	26,2	0,33
P1	cKO	282	1,48	1,05	28,8	0,37
P5	CTRL	460	1,46	0,81	44,7	0,48
P5	CTRL	510	1,53	0,75	51,2	0,43
P5	CTRL	486	1,79	1,17	34,5	0,31
P5	CTRL	505	1,88	1,10	41,5	0,46
P5	CTRL	536	1,77	0,90	49,2	0,45
P5	CTRL	455	1,42	0,76	46,2	0,46
P5	cKO	581	2,89	2,78	3,8	0,43
P5	cKO	492	3,40	3,08	9,4	0,37
P5	cKO	410	3,84	3,68	4,0	0,35
P5	cKO	321	3,10	2,85	7,9	0,45
P5	cKO	302	2,59	2,30	11,2	0,31
P10	CTRL	453	1,59	1,03	35,4	0,39
P10	CTRL	531	1,36	0,66	51,3	0,47
P10	CTRL	520	1,55	0,79	48,8	0,42
P10	CTRL	484	1,96	1,03	47,7	0,41
P10	CTRL	513	1,65	0,79	51,9	0,52
P10	cKO	421	4,21	4,18	0,6	0,38
P10	cKO	507	4,07	3,83	6,0	0,42
P10	cKO	422	4,35	4,15	4,8	0,31
P10	cKO	543	4,29	4,14	3,6	0,34
P10	cKO	474	3,85	3,65	5,2	0,35

Supplemental Table 4. List of Ca^{2+}-binding proteins detected by mass spectrometry analysis.

Gene name	Protein name	Species
Casq1	**Calsequestrin-1**	**Mus musculus**
Ryr2	**Ryanodine receptor 2**	**Mus musculus**
Ttn	**Titin**	**Mus musculus**
Atp2a2	**Sarcoplasmic/endoplasmic reticulum calcium ATPase 2**	**Mus musculus**
Anxa11	**Annexin A11**	**Mus musculus**
Slc25a12	**Calcium-binding mitochondrial carrier protein Aralar1**	**Mus musculus**
Nid2	**Nidogen-2**	**Mus musculus**
Anxa4	**Annexin A4**	**Mus musculus**
Apcs	**Serum amyloid P-component**	**Mus musculus**
Rcn2	**Reticulocalbin-2**	**Mus musculus**
Anxa1	**annexin A1**	**Mus musculus**
Itih1	**Inter-alpha-trypsin inhibitor heavy chain H1**	**Mus musculus**

Supplemental Figures

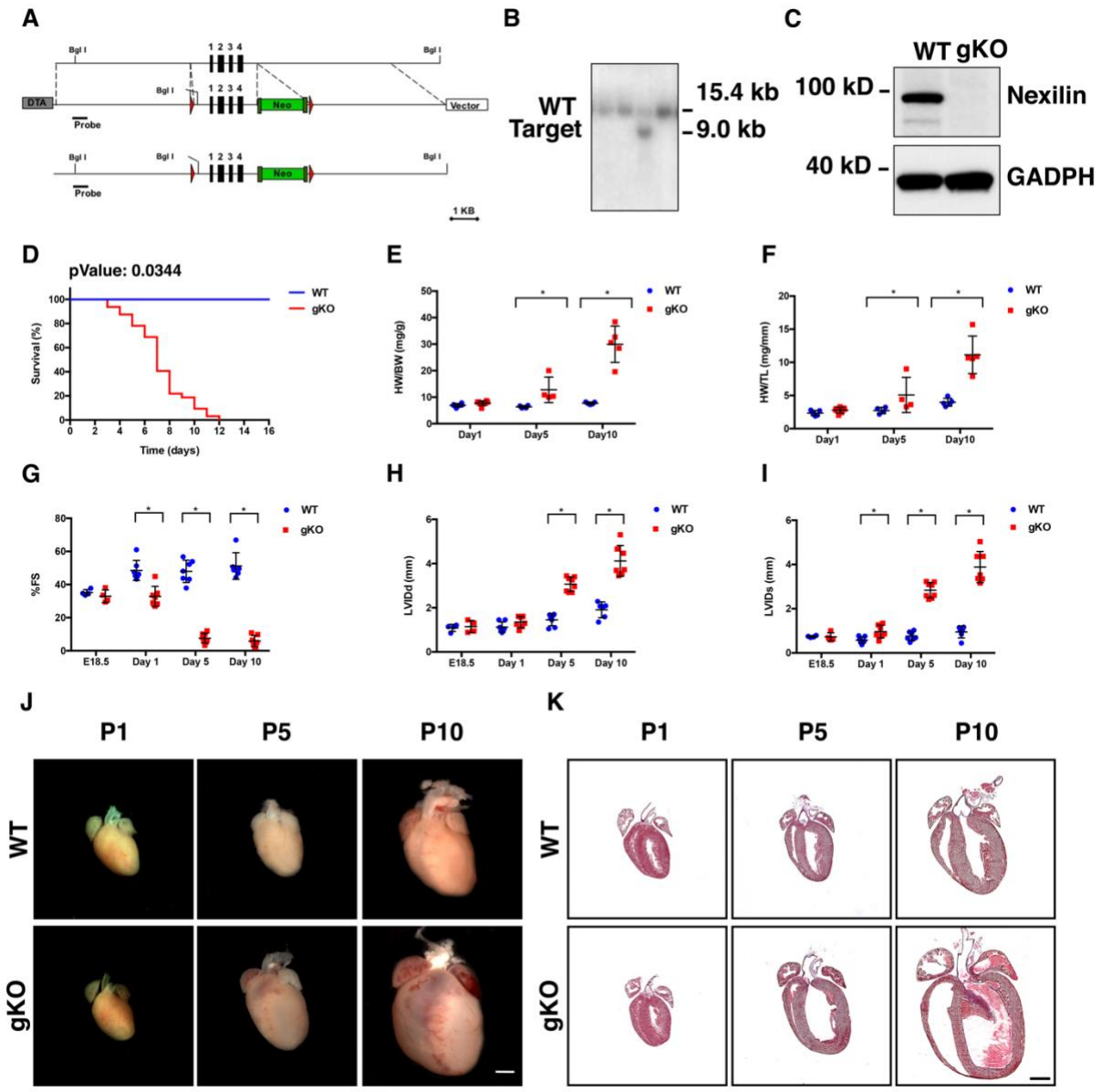

Supplemental Figure 1. Global loss of NEXN leads to progressive and severe dilated cardiomyopathy. (**A-C**), Generation of NEXN floxed mice: (**A**) restriction map of the relevant genomic region of NEXN (top), targeting construct (middle), and the mutated locus following recombination (bottom) (DTA, Diphtheria Toxin A chain gene; Neo, neomycin resistance gene); (**B**) Detection WT and mutant (Target) alleles by Southern blot analysis, following digestion with Bgl I; (**C**) Detection of NEXN expression in WT and gKO heart by Western blot. (**D**) Kaplan-Meier survival curves for WT (n = 30) and gKO (n = 32) mice; (**E-F**), Graphs representing (**E**) HW/BW (n=5-6 mice per time point) and (**F**) HW/TL (n=5-6 mice per time point). (**G-I**) graphs representing echocardiographic measurements from WT and gKO mice (n = 4-7 mice per time point): (**G**) % FS, (**H**) Left ventricular internal diameter end-diastole (LVIDd) and (**I**) Left ventricular internal diameter end-systole (LVIDs). (**J**) Representative whole heart images from postnatal day 1 (P1), 5 (P5) or 10 (P10) mice. (**K**) Representative 4-chambers view Masson's trichrome staining images of longitudinal histological heart sections. (J-K) Scale bars 1mm. (*****) Statistically significant differences with P value < 0.05. Average HRs (bpm): WT (E18.5) 334±20, (P1) 342±68, (P5) 484±81, (P10) 523±49; gKO (E18.5) 329±34, (P1) 365±72, (P5) 456±50, (P10) 371±145.

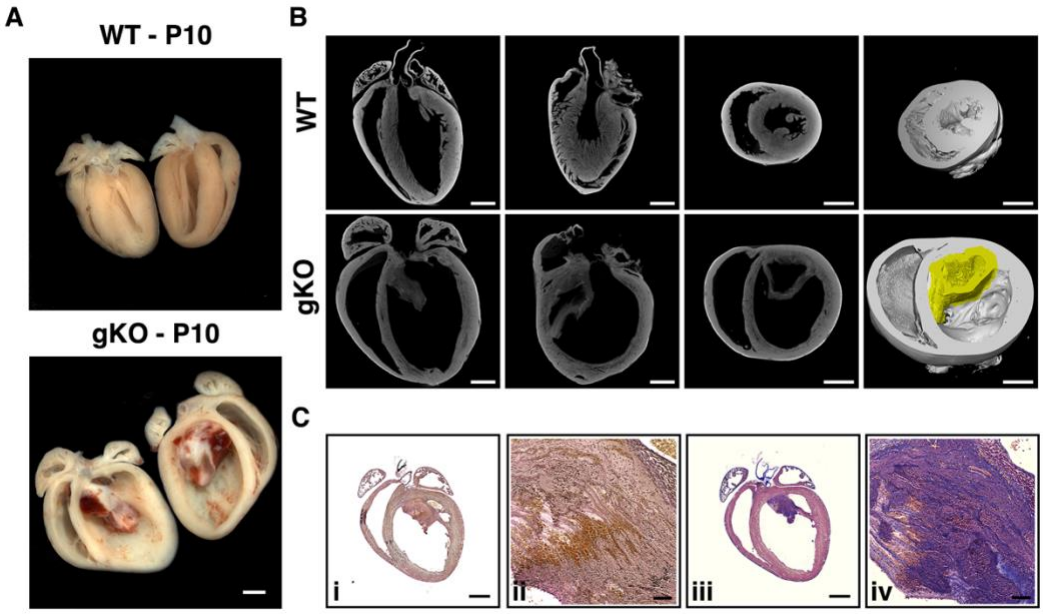

Supplemental Figure 2. Intracardiac thrombus in dilated NEXN gKO hearts. (**A**) Representative butterfly cut gross anatomy images of P10 mouse hearts revealing an organized formation in the left ventricle of the *Nexn*$^{-/-}$ (gKO) heart. (**B**) Representative micro-CT images of P10 mouse hearts; from left to right: longitudinal, sagittal, transversal, or tridimensional view. (**C**) Representative histological pictures showing the absence of elastic fibers and the presence of collagen and fibrin, allowing us to classify the formation as an intracardiac organized mural thrombus: (i) Vernhoff Van Gieson and (iii) Carstairs' staining of 4-chambers view longitudinal sections from P10 *Nexn*$^{-/-}$ mouse heart with related high magnifications (ii, iv). Scale bars (i, iii) 1mm and (ii, iv) 100µm.

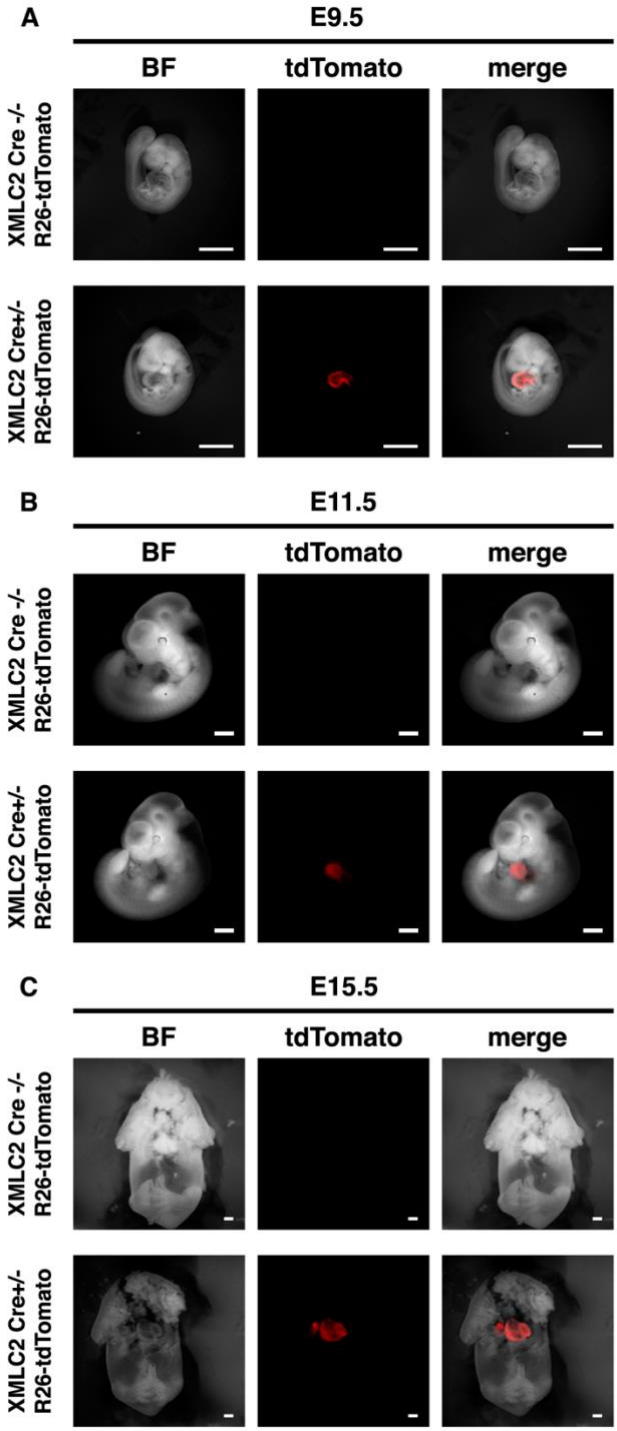

Supplemental Figure 3. The cardiac specific Cre recombinase activity of Xenopus laevis myosin light-chain 2-Cre mice. (**A-C**) Representative pictures showing XMLC2-Cre expression specificity for heart tissue from embryos (**A**) 9.5, (**B**) 11.5 and (**C**) 15.5 days of XMLC2-Cre; R26-tdTomato mice. Scale bars: 1mm.

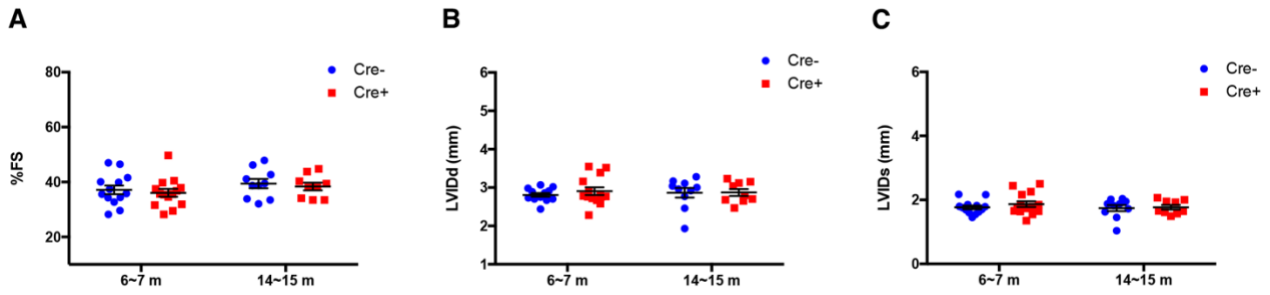

Supplemental Figure 4. Echocardiographic analysis of Xenopus laevis myosin light-chain 2-Cre mice. (**A-C)** Graphs representing echocardiographic measurements from WT and Xenopus laevis myosin light-chain 2-Cre mice (n = 10 mice per time point, where m=months): (**A**) % FS, (**B**) LVIDd and (**C**) LVIDs. Average HRs (bpm): (Cre-) 640±43; (Cre+) 659±41 .

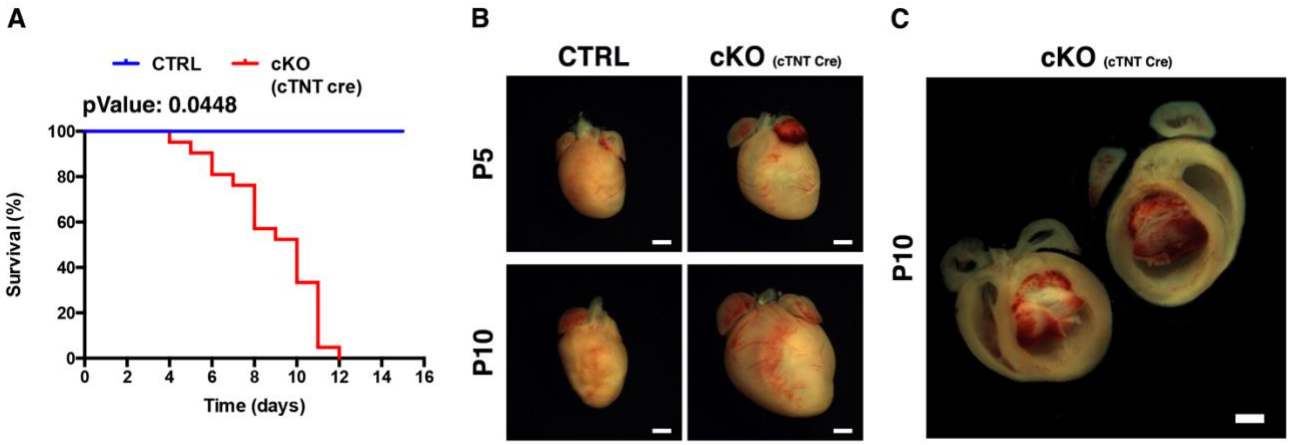

Supplemental Figure 5. Phenotype evaluation of troponin T2-cre NEXN$^{f/f}$ mice. (**A**) Kaplan-Meier survival curves for *Nexn* control (CTRL, n = 35) and troponin T2-cre *Nexn*$^{f/f}$ cardiomyocytes specific KO (cKO cTNT cre, n = 24) mice. (**B**) Representative whole heart images of P5 and P10 cKO cTNT cre mice and littermates CTRLs. (**C**) Representative butterfly cut gross anatomy images of a P10 cKO cTNT cre mouse heart revealing an organized formation in the left ventricle resembling those found in *Nexn*$^{-/-}$ P10 hearts. (B-C) Scale bars: 1mm.

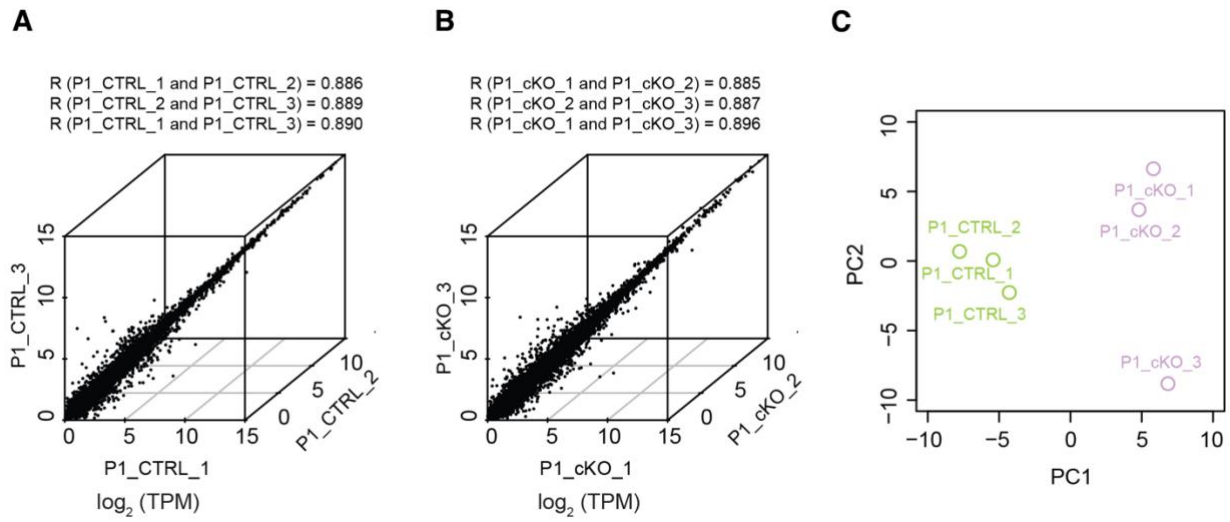

Supplemental Figure 6. Quality control of RNA-seq data. (**A**-**B**) Comparison of the gene expression quantified as TPM between replicates for (**A**) CTRL or (**B**) cKO RNA-seq data. Spearman correlation coefficients are indicated. (**C**) PCA analysis of RNA-seq data. CTRL and cKO samples are labeled in light green and light purple respectively.

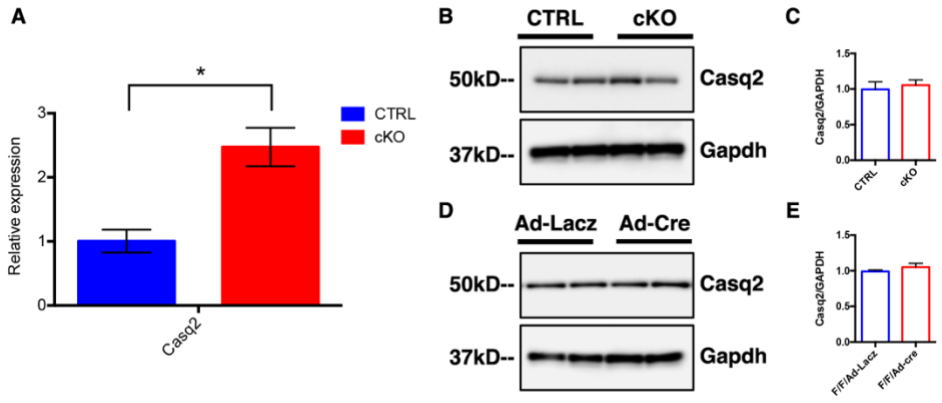

Supplemental Figure 7. Expression of Calsequestrin 2 in Nexn cKO heart. (**A**) qPCR analysis of Calsequestrin 2(Casq2) from E18.5 mouse ventricles (n = 4). Western blot representative images and (**B**) quantification graphs of Casq2 from (**C**) E18.5 mouse ventricles (n = 4) and from (**D-E**) isolated neonatal NEXN$^{f/f}$ cardiomyocytes treated with Ad-Lacz or Ad-cre virus (n=6). (*) Statistically significant differences with P value < 0.05.

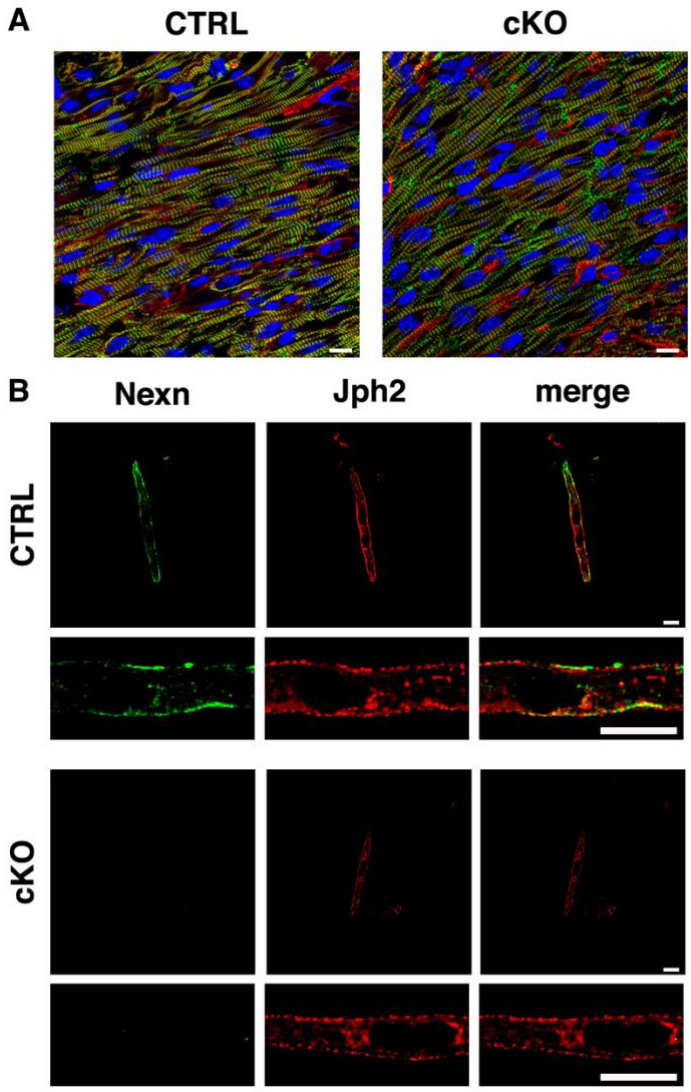

Supplemental Figure 8. NEXN does not localize in the Z-disc of P5 cardiomyocytes and sarcomere structure is not altered by loss of NEXN. (**A**) Representative confocal images showing no alterations in the sarcomere organization of a P5 *Nexn* cKO heart: myomesin in red, α-actinin in green and DAPI in blue for nuclei. (**B**) Representative confocal images of P5 *Nexn* cKO cardiomyocytes: no positive signal detected for NEXN in the cKO, high magnification images of the CTRL cardiomyocytes showing again NEXN localization with Jph2. Scale bars 10μm.

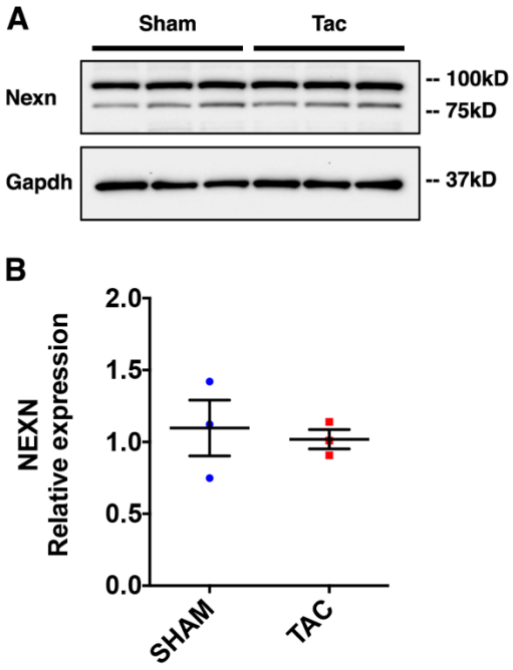

Supplemental Figure 9. NEXN protein level in induced heart disease mouse model. (**A**) Representative western blot images of NEXN protein level in a TAC mouse model. (B) Relative quantification.

References

1. Liang X, Zhou Q, Li X, Sun Y, Lu M, Dalton N, Ross J, Jr. and Chen J. PINCH1 plays an essential role in early murine embryonic development but is dispensable in ventricular cardiomyocytes. *Mol Cell Biol*. 2005;25:3056-62.
2. Fang X, Stroud MJ, Ouyang K, Fang L, Zhang J, Dalton ND, Gu Y, Wu T, Peterson KL, Huang HD, Chen J and Wang N. Adipocyte-specific loss of PPARgamma attenuates cardiac hypertrophy. *JCI Insight*. 2016;1:e89908.
3. Wagner E, Brandenburg S, Kohl T and Lehnart SE. Analysis of tubular membrane networks in cardiac myocytes from atria and ventricles. *J Vis Exp*. 2014:e51823.
4. Schindelin J, Arganda-Carreras I, Frise E, Kaynig V, Longair M, Pietzsch T, Preibisch S, Rueden C, Saalfeld S, Schmid B, Tinevez JY, White DJ, Hartenstein V, Eliceiri K, Tomancak P and Cardona A. Fiji: an open-source platform for biological-image analysis. *Nat Methods*. 2012;9:676-82.
5. Patro R, Duggal G, Love MI, Irizarry RA and Kingsford C. Salmon provides fast and bias-aware quantification of transcript expression. *Nat Methods*. 2017;14:417-419.
6. Love MI, Huber W and Anders S. Moderated estimation of fold change and dispersion for RNA-seq data with DESeq2. *Genome Biol*. 2014;15:550.
7. Zhu A, Ibrahim JG and Love MI. Heavy-tailed prior distributions for sequence count data: removing the noise and preserving large differences. *Bioinformatics*. 2018.
8. Reynolds JO, Chiang DY, Wang W, Beavers DL, Dixit SS, Skapura DG, Landstrom AP, Song LS, Ackerman MJ and Wehrens XH. Junctophilin-2 is necessary for T-tubule maturation during mouse heart development. *Cardiovasc Res*. 2013;100:44-53.